Geophysical Prospecting

EAGE EUROPEAN ASSOCIATION OF GEOSCIENTISTS & ENGINEERS

Geophysical Prospecting, 2010, 58, 429–439 doi: 10.1111/j.1365-2478.2009.00845.x

Kinematic characteristics and the influence of reference velocities of phase-shift-plus-interpolation and extended-split-step-Fourier migration methods

Jing-Bo Chen[1]* and Shu-Yuan Du[1,2]

[1]*Key Laboratory of Petroleum Geophysics, Institute of Geology and Geophysics, Chinese Academy of Sciences, PO Box 9825, Beijing 100029, China, and* [2]*Graduate University of Chinese Academy of Sciences, Beijing 100049, China*

Received April 2009, revision accepted August 2009

ABSTRACT

The phase-shift-plus-interpolation and extended-split-step-Fourier methods are wavefield-continuation algorithms for seismic migration imaging. These two methods can be applied to regions with complex geological structures. Based on their unified separable formulas, we show that these two methods have the same kinematic characteristics by using the theory of pseudodifferential operators. Numerical tests on a Marmousi model demonstrate this conclusion. Another important aspect of these two methods is the selection of reference velocities and we explore the influence of the selection of reference velocities by comparing the geometric progression method and the statistical method. We show that the geometric progression method is simple but does not take into account the velocity distribution while the statistical approach is relatively complex but reflects the velocity distribution.

INTRODUCTION

Seismic migration is a wave-equation-based process that creates the image of structures within the earth form recorded data on the surface. Historically, it was a process of moving reflection events to their true positions by collapsing diffraction events on unmigrated sections. With its scope increasingly broadening, seismic migration has now become a central step in seismic data processing (Gray *et al.* 2001).

Seismic migration algorithms can be classified into two categories: integral methods and wavefield-continuation methods (Biondi 2006). Wavefield-continuation methods are more suited to regions with complex geology. We will consider two kinds of wavefield-continuation methods: phase-shift-plus-interpolation (PSPI) (Gazdag and Sguazzero 1984) and extended-split-step-Fourier methods (Kessinger 1992; Biondi 2006). These two methods belong to separable approximations of a one-way wave operator (Chen and Liu 2004, 2006; Ferguson and Margrave 2005; Chen, Liu and Zhang 2007). In this paper, we will develop unified separable formulas for these two methods, which enable us to obtain a clear understanding of their separable properties.

In the PSPI method, a time-shift is applied to the initial wavefield before wavefield continuation, whereas in the extended-split-step-Fourier method, the time-shift is applied after the wavefield is continued with a background velocity. The relationship between these two methods can be explained by the theory of pseudodifferential operators. In this framework, the two methods can be interpreted as two different pseudodifferential operators. These two operators have the same characteristics and therefore describe the same kinematic properties for wave propagation. This accounts for their similar imaging effects in terms of the position and shape of the geological structure.

For both methods, the selection of reference velocities is needed. One approach was presented in Gazdag and Sguazzero (1984). The reference velocities are obtained in terms of the ratio of maximum velocity and minimum velocity at some depth as well as a common ratio for which a geometric progression for reference velocities is formed. Another statistical method for determining the reference velocities was suggested by Bagaini, Bonomi and Pieroni (1995). An implementation program of the statistical method is available

*E-mail: chenjb@vip.sohu.com

(Han 1998). For the statistical method, the velocity interval between the maximum and minimum velocities of the velocity model is divided into L subintervals and then the reference velocities at some depth are determined by the distribution of the velocities at that depth. In this paper, we will make a comparison of the geometrical progression and the statistical methods.

In the next section, we will briefly review the concept of separable approximation for the one-way wave operator. Then we will present the separable formulations for the PSPI and extended-split-step-Fourier methods. This is followed by an analysis of their relationship. We then discuss the issue of selecting reference velocities. Finally, we perform some numerical experiments to demonstrate the theoretical analysis.

SEPARABLE APPROXIMATION FOR ONE-WAY WAVE OPERATOR

To begin with, we recall the concept of separable approximation for the one-way wave operator (Chen and Liu 2004, 2006; Chen *et al.* 2007).

Consider the one-way wave operator in frequency-wavenumber domain

$$\mathcal{A}(x, y; k_x, k_y) = \exp\left\{ \mathrm{i}\sqrt{\frac{\omega^2}{v(x, y, \bar{z})^2} - (k_x^2 + k_y^2)}\,\Delta z \right\}, \qquad (1)$$

where ω is circular frequency, k_x, k_y are wavenumbers, v is the velocity, Δz is the continuation depth and $\bar{z} = z + \frac{1}{2}\Delta z$.

The separable approximation for the one-way operator (1) is

$$\mathcal{A}(x, y; k_x, k_y) \sim \sum_{j=1}^{s} f_j(x, y) g_j(k_x, k_y), \qquad (2)$$

where $f_j(x, y)\,(j = 1, 2, \ldots, s)$ are functions in x and y only, $g_j(k_x, k_y)\,(j = 1, 2, \ldots, s)$ are functions in k_x and k_y only and s refers to the order of the separable approximation.

The wavefield-continuation formula can be written in the following form

$$U(z + \Delta z, x, y) = \frac{1}{4\pi^2} \int [\mathcal{A}(x, y; k_x, k_y)\tilde{U}(z, k_x, k_y)] \times \exp\{\mathrm{i}(xk_x + yk_y)\}\mathrm{d}k_x\mathrm{d}k_y, \qquad (3)$$

where $U(x, y, z)$ is the wavefield and $\tilde{U}(k_x, k_y, z)$ is its Fourier transform with respect to x and y.

The inverse Fourier transform in equation (3) depends on the spatial variables x and y and therefore the FFT alogrithm can not be applied directly.

Using the separable approximation (2), formula (3) becomes

$$U(z + \Delta z, x, y) = \frac{1}{4\pi^2} \sum_{j=1}^{s} \left[f_j(x, y) \int g_j(k_x, k_y)\tilde{U}(z, k_x, k_y)] \times \exp\{\mathrm{i}(xk_x + yk_y)\}\mathrm{d}k_x\mathrm{d}k_y \right]. \qquad (4)$$

Based on equation (4), we can use FFT to greatly improve computational efficiency.

There are two kinds of separable approximations: local separable approximations (such as the split-step Fourier method (Stoffa *et al.* 1990) and the generalized-screen method (Le Rousseau and de Hoop 2001) and global separable approximations (such as the optimal separable approximation (Chen and Liu 2004, 2006). For details, see Chen and Liu (2006). In the next section, we will show that the PSPI and extended-split-step-Fourier methods are both separable approximations.

SEPARABLE APPROXIMATION FOR PHASE-SHIFT-PLUS-INTERPOLATION AND EXTENDED-SPLIT-STEP-FOURIER METHODS

Phase-shift-plus-interpolation (PSPI) method The PSPI method was proposed by Gazdag and Sguazzero (1984). It consists of phase-shift wavefield continuation with constant reference velocity and interpolation between different wavefilelds continued with different reference velocities. In this method, a time-shift term is first applied to the initial wavefield before wavefield continuation.

To gain a deep understanding of the PSPI method as a whole, we need to derive a unified formula that accounts for the three steps of PSPI: 1) a time-shift term applied to the initial wavefield; 2) phase-shift with reference velocities and 3) interpolation between wavefileds. This unified formula was not proposed in Gazdag and Sguazzero (1984). Ferguson and Margrave (2005) suggested an approximately unified formula. However, their formula does not give the time-shift term and the interpolation factors explicitly. Here, we will derive a unified formula of PSPI that is in the form of separable approximation. This formula is important for us to understand the kinematic characteristic of the PSPI method.

Suppose that there are n reference velocities:

$$v_{min} = v_1 < v_2 < \cdots < v_{n-1} < v_n = v_{max}.$$

The unified separable approximation for PSPI reads:

$$\mathcal{A}(x, y; k_x, k_y) \sim \sum_{j=1}^{n} h_j(x, y) \overrightarrow{\exp\left\{\mathrm{i}\frac{\omega}{v(x, y)}\Delta z\right\}} \times \exp\left\{\mathrm{i}\left(\sqrt{\frac{\omega^2}{v_j^2} - k_x^2 - k_y^2} - \frac{\omega}{v_j}\right)\Delta z\right\}, \quad (5)$$

where $h_j(x, y)$ $(j = 1, 2, \ldots, n)$ are interpolation factors with the following form:

$$h_1(x, y) = \begin{cases} \frac{v_2 - v(x,y)}{v_2 - v_1}, & v_1 \leqslant v(x, y) < v_2, \\ 0, & \text{otherwise.} \end{cases}$$

$$h_j(x, y) = \begin{cases} \frac{v(x,y) - v_{j-1}}{v_j - v_{j-1}}, & v_{j-1} \leqslant v(x, y) < v_j, \\ \frac{v_{j+1} - v(x,y)}{v_{j+1} - v_j}, & v_j \leqslant v(x, y) < v_{j+1}, \\ 0, & \text{otherwise.} \end{cases} \quad \text{for} \quad j = 2, 3, \ldots, n-1.$$

$$h_n(x, y) = \begin{cases} \frac{v(x,y) - v_{n-1}}{v_n - v_{n-1}}, & v_{n-1} \leqslant v(x, y) \leqslant v_n, \\ 0, & \text{otherwise.} \end{cases}$$

Here the arrow in the term $\overrightarrow{\exp\left\{\mathrm{i}\left(\frac{\omega}{v(x, y)}\right)\Delta z\right\}}$ indicates that when the one-way operator applies to a wavefield, this term first multiplies with the wavefield. In Gazdag and Sguazzero (1984), the interpolation is performed on the amplitude and phase of the wavefileds separately. Here we consider the interpolation applied directly to the wavefields. According to our experience, these two methods of interpolation produce similar results.

The approximation (5) can be rewritten as

$$\mathcal{A}(x, y; k_x, k_y) \sim \sum_{j=1}^{n} f_j(x, y) g_j(k_x, k_y), \quad (6)$$

where

$$f_j(x, y) = h_j(x, y), \quad j = 1, 2, \ldots, n,$$

$$g_j(k_x, k_y) = \overrightarrow{\exp\left\{\mathrm{i}\left(\frac{\omega}{v(x, y)}\right)\Delta z\right\}} \times \exp\left\{\mathrm{i}\left(\sqrt{\frac{\omega^2}{v_j^2} - k_x^2 - k_y^2} - \frac{\omega}{v_j}\right)\Delta z\right\}.$$

Therefore, PSPI is a separable approximation.

Extended-split-step-Fourier (ESSF) method The extended-split-step-Fourier method was first proposed by Kessinger (1992). The multiple reference velocity logic of PSPI is applied to the split-step Fourier method but no interpolation is conducted. Biondi (2006) added the interpolation step to the extended-split-step-Fourier method, which is the extended-split-step-Fourier method we consider in this paper. Therefore the extended-split-step-Fourier method under consideration here also consists of phase shift and interpolation. Its difference with PSPI is that the time-shift is applied after wavefield continuation instead of before wavefield continuation. Now we derive the unified separable approximation for ESSF.

Suppose that there are n reference velocities:

$$v_{min} = v_1 < v_2 < \cdots < v_{n-1} < v_n = v_{max}.$$

The unified separable approximation for extended-split-step-Fourier reads:

$$\mathcal{A}(x, y; k_x, k_y) \sim \sum_{j=1}^{n} h_j(x, y) \exp\left\{\mathrm{i}\left(\frac{\omega}{v(x, y)} - \frac{\omega}{v_j}\right)\Delta z\right\} \times \exp\left\{\mathrm{i}\sqrt{\frac{\omega^2}{v_j^2} - k_x^2 - k_y^2}\,\Delta z\right\}. \quad (7)$$

where $h_j(x, y)$ $(j = 1, 2, \ldots, n)$ are the same interpolation factors as in equation (5). The approximation (7) can be rewritten as

$$\mathcal{A}(x, y; k_x, k_y) \sim \sum_{j=1}^{n} f_j(x, y) g_j(k_x, k_y). \quad (8)$$

where

$$f_j(x, y) = h_j(x, y) \exp\left\{\mathrm{i}\left(\frac{\omega}{v(x, y)} - \frac{\omega}{v_j}\right)\Delta z\right\},$$

$$g_j(k_x, k_y) = \exp\left\{\mathrm{i}\sqrt{\frac{\omega^2}{v_j^2} - k_x^2 - k_y^2}\,\Delta z\right\}.$$

Therefore, ESSF is indeed a separable approximation.

RELATIONSHIP BETWEEN PHASE-SHIFT-PLUS-INTERPOLATION AND EXTENDED-SPLIT-STEP-FOURIER METHODS

Now we explore the relationship between PSPI and extended-split-step-Fourier (ESSF) based on the theory of pseudodifferential operators. See the Appendix for some basic facts on pseusodifferential operators that will be needed in the following development.

We set

$$L(\boldsymbol{x}, \boldsymbol{p}; \omega) = \exp\left\{\mathrm{i}\left(\frac{\omega}{v(x, y)} - \frac{\omega}{v_j}\right)\Delta z\right\} \times \exp\left\{\mathrm{i}\sqrt{\frac{\omega^2}{v_j^2} - k_x^2 - k_y^2}\,\Delta z\right\}, \quad (9)$$

where $\boldsymbol{x} = (x_1, x_2) = (x, y)$ and $\boldsymbol{p} = (p_1, p_2) = (k_x, k_y)$.

Based on equation (9), we can define two operators:

$$L(\overset{1}{\boldsymbol{x}}, \overset{2}{D}_x; \omega)u(\boldsymbol{x}) = F_{p\to x}^{-1}\left[\exp\left\{\mathrm{i}\left(\sqrt{\frac{\omega^2}{v_j^2} - k_x^2 - k_y^2} - \frac{\omega}{v_j}\right)\Delta z\right\} \times F_{x\to p}\left(\exp\left\{\mathrm{i}\frac{\omega}{v(x, y)}\Delta z\right\}u(\boldsymbol{x})\right)\right], \quad (10)$$

$$L(\overset{2}{\boldsymbol{x}}, \overset{1}{D}_x; \omega)u(\boldsymbol{x}) = \exp\left\{\mathrm{i}\left(\frac{\omega}{v(x, y)} - \frac{\omega}{v_j}\right)\Delta z\right\} \times F_{p\to x}^{-1}\left[\exp\left\{\mathrm{i}\sqrt{\frac{\omega^2}{v_j^2} - k_x^2 - k_y^2}\,\Delta z\right\}F_{x\to p}u(\boldsymbol{x})\right], \quad (11)$$

where $u(\boldsymbol{x})$ is the wavefield to be continued downward. See the appendix for the meaning of the notations in equations (10) and (11).

The operators defined in equations (10) and (11) correspond to the separable formulations for the PSPI (equation (5)) and the extended-split-step-Fourier (equation (7)) respectively when they are applied to a wavefield. The two operators (10) and (11) have the same characteristics, i.e., the same traveltime function (see the appendix). Therefore, the PSPI and ESSF methods have the same kinematic imaging effect, but the dynamics they describe are different. It should be noted that the one-way wave operator (1) only describes the kinematic characteristics of wave propagation and does not account for the dynamic characteristics of wave propagation correctly (Le Rousseau and de Hoop 2001). Therefore, as approximations of operator (1), neither PSPI nor extended-split-step-Fourier gives a correct description of dynamics of wave propagation. In order to account for both kinematics and dynamics, a true-amplitude one-way operator is needed. The true-amplitude one-way operator is a modified version of equation (1). For details, see Zhang, Zhang and Bleistein (2005).

SELECTION OF REFERENCE VELOCITIES

An important issue in implementing PSPI and extended-split-step-Fourier is the selection of reference velocities. There are two approaches available: geometric progression method (Gazdag and Sguazzero 1984) and the statistical method (Bagaini *et al.* 1995; Han 1998). We will present these two methods and give some theoretical analysis. For simplicity, we will only consider the two-dimensional case. In the next section, we will perform some numerical comparisons in the case of the Marmousi model.

Geometric progression method (Gazdag and Sguazzero 1984). Let R denote the ratio of the maximum velocity v_{max} and the minimum velocity v_{min} at some depth and let ρ denote the common ratio for which the consecutive reference velocities form a geometric progression (see below). The number of reference velocities m is determined by the smallest integer satisfying

$$\rho^{m-1} \geqslant R. \quad (12)$$

Therefore, we obtain

$$m = \begin{cases} \frac{\ln R}{\ln \rho} + 1, & \text{if } \frac{\ln R}{\ln \rho} \text{ is an integer,} \\ \left\lfloor \frac{\ln R}{\ln \rho} + 1 \right\rfloor + 1, & \text{if } \frac{\ln R}{\ln \rho} \text{ is not an integer,} \end{cases}$$

where $\lfloor \cdot \rfloor$ denotes the integer part of a real number.

Then the consecutive reference velocities are chosen as

$$v_1, v_2, \ldots, v_{m-1}, v_m, \quad \text{where } v_1 = v_{min}, \quad \text{and } \frac{v_{i+1}}{v_i} = \rho, i = 1, 2, \ldots, m-1.$$

Based on the above definition of m, we have

$$v_{max} \leqslant v_m < \rho\, v_{max}.$$

Statistical method (Bagaini *et al.* 1995; Han 1998). Let v_{min} and v_{max} denote the minimum and maximum velocities in the velocity model, respectively. We set

$$c_i = v_{min} + i(v_{max} - v_{min})/L, \quad i = 0, 1, 2, \ldots, L,$$

where L is an integer. Then the interval $[v_{min}, v_{max}]$ is divided into L subintervals:

$$\left[c_0, c_1\right), \left[c_1, c_2\right), \ldots, \left[c_{L-2}, c_{L-1}\right), \left[c_{L-1}, c_L\right].$$

Suppose that there are n_x lateral velocities $v(x_l, z)(l = 1, 2, \ldots, n_x)$ at some depth. These velocities will fall into one of the above L subintervals. Let n_i denote the number of the velocities that fall into the interval $[\, c_i, c_{i+1})$, $(i = 0, 1, \ldots, L-2)$ and n_{L-1} the number of the velocities falling into the interval$[\, c_{L-1}, c_L\,]$.

Let $P_i = n_i/n_x, \quad i = 0, 1, \ldots, L-1$. Note that $0 \leqslant P_i \leqslant 1$ and $\sum_{i=0}^{L-1} P_i = 1$. Then we construct a number:

$$B = \exp\left[\sum_{P_i \neq 0} \ln P_i^{-P_i}\right] = \prod_{P_i \neq 0} P_i^{-P_i}. \tag{13}$$

Now we recall a well-known inequality (Hardy, Littlewood and Pólya 1952):

$$a_1^{P_1} a_2^{P_2} \cdots a_n^{P_n} \leqslant \left(\frac{P_1 a_1 + P_2 a_2 + \cdots + P_n a_n}{P_1 + P_2 + \cdots + P_n}\right)^{P_1+P_2+\cdots+P_n}, \tag{14}$$

where $a_i > 0, P_i > 0, \quad (i = 1, 2, \ldots, n)$ and the equality holds only when $a_1 = a_2 = \ldots = a_n$. Using the inequality (14) and noting that $0 \leqslant P_i \leqslant 1$ and $\sum_{i=0}^{L-1} P_i = 1$, we can easily prove that the number in equation (13) satisfies

$$1 \leqslant B \leqslant L. \tag{15}$$

Finally, the number of the reference velocities is chosen as

$$m = \lfloor B + 0.5 \rfloor + 1, \tag{16}$$

where $\lfloor \cdot \rfloor$ again denotes the integer part of a real number.

Using the inequality (15), we can obtain

$$2 \leqslant m \leqslant L + 1. \tag{17}$$

To determine the reference velocities, we set $Y_0 = 0$ and $Y_j = \sum_{i=0}^{j-1} P_i, \quad j = 1, 2, \ldots, L$. We then set $v_0 = v_{min}$ and if there exits some j such that $Y_j < i/(m-1) \leqslant Y_{j+1}$, then the reference velocity is determined as follows

$$v_i = c_j + \frac{i/(m-1) - Y_j}{Y_{j+1} - Y_j}(c_{j+1} - c_j), \quad i = 1, 2, \ldots, m-1. \tag{18}$$

Then we have the m reference velocities

$$v_0, v_1, \ldots, v_{m-1}.$$

Based on equation (18) and the definition of Y_j, we can conclude that $v_{m-1} = c_{j+1}$. Let lv_{max} denote the maximum velocity within the depth under consideration. If $lv_{max} = v_{max}$, then $v_{m-1} = c_{j+1} = v_{max}$ and if $lv_{max} < v_{max}$, then $v_{m-1} = c_{j+1} > lv_{max}$.

In the Han's program, the reference velocity v_{m-1} is slightly modified by $\tilde{v}_{m-1} = 1.005 v_{m-1}$. The purpose of this modification is just to make the subsequent interpolation implementation more convenient.

NUMERICAL EXPERIMENTS

In this section, we will perform some numerical experiments. First, we compare the two methods of selecting reference velocities. Second, we compare the imaging effect of PSPI and extended-split-step-Fourier. In both numerical examples, we use the Marmousi model.

For both methods for selecting reference velocities, when the ratio of the maximum and minimum velocities at some

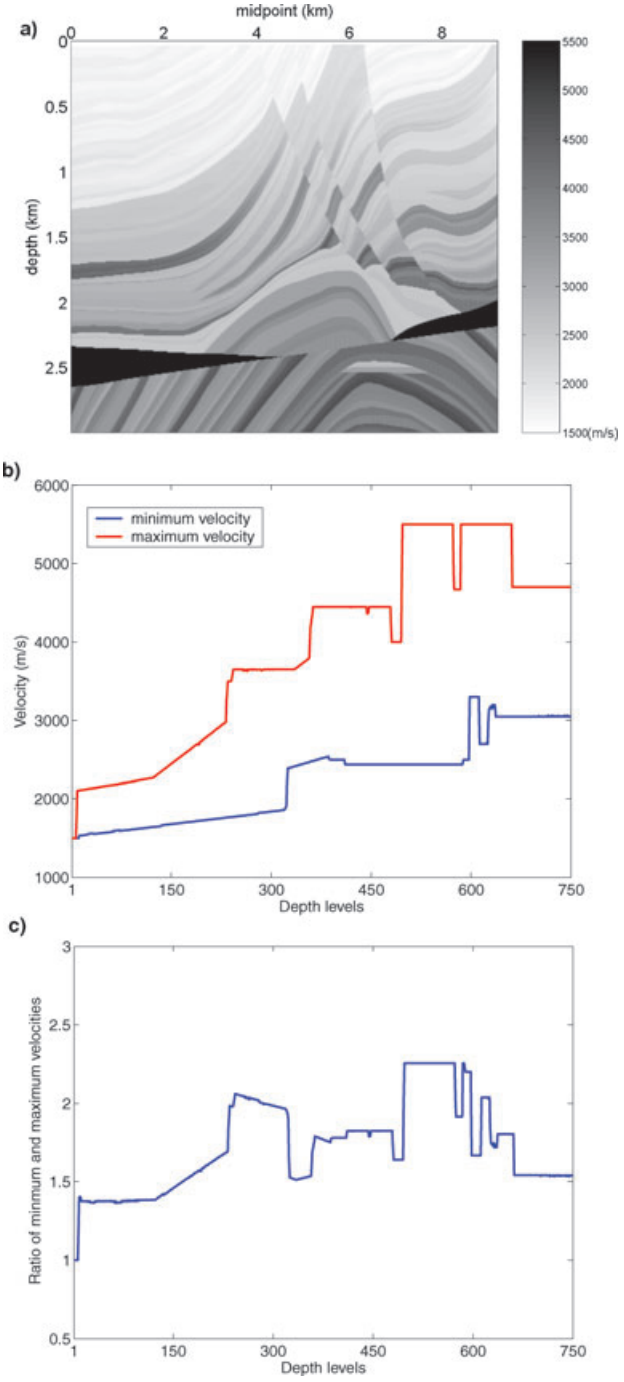

Figure 1 The Marmousi velocity model (a). The minimum and maximum velocities for depth levels (b). The ratio of maximum and minimum velocities for depth levels (c).

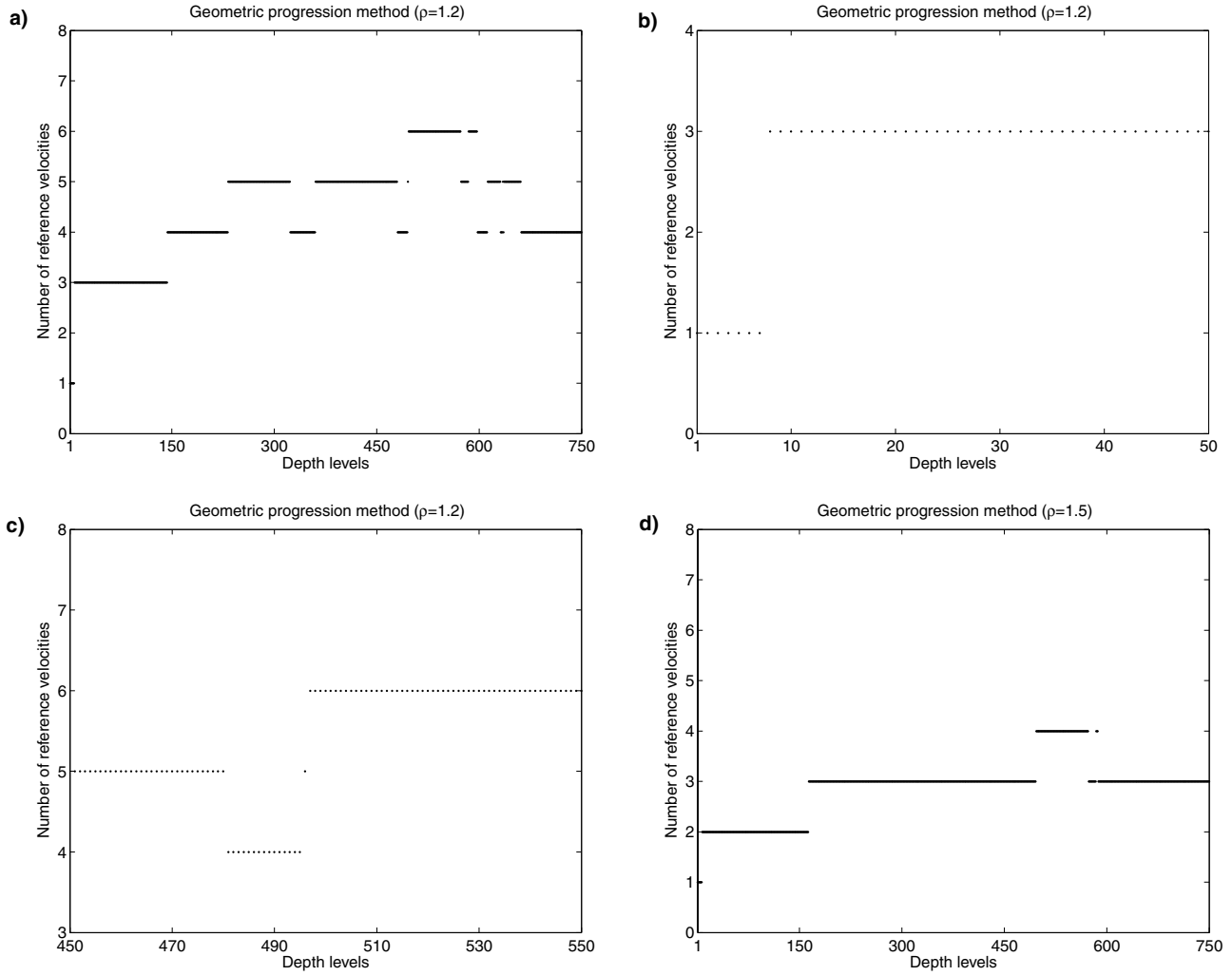

Figure 2 Geometrical progression method for selecting reference velocities. (a) The result for $\rho = 1.2$; (b) and (c) are the enlarged portion of (a); (d) the result for $\rho = 1.5$.

depth is less than some upper bound B, we will use only one reference and no interpolation is needed. In our experiments, we will choose $B = 1.01$ as used in the Han's program.

The Marmousi model consists of in a 750 by 737 velocity matrix (a simplified version) (Fig. 1a). The maximum velocity is 5500 m/s and the minimum velocity is 1500 m/s. The maximum and minimum velocities and their ratio for different depth levels are displayed in Figs 1(b) and 1(c), respectively. The maximum ratio is about 2.25.

We first examine the geometrical progression method. We first set $\rho = 1.2$. Figure 2(a) shows the number of reference velocities for different depth levels. Figure 2(b,c) is the enlarged portion of Fig. 2(a). For the first 7 depth levels, the ratio of maximum and minimum velocities is less than $B = 1.01$ and therefore there is only one reference velocity. For other depth levels, the number of reference velocities is larger than 1 and the maximum number of reference velocities is 6. The number of reference velocities will decrease with increasing ρ. Figure 2(d) shows the corresponding result for $\rho = 1.5$.

Now we explore the statistical approach. We first choose $L = 10$. Figure 3(a) shows the number of reference velocities for different depth levels. In this case, the maximum number of reference velocities is 7. The number of reference velocities will increase with increasing L. The corresponding results for $L = 5$ and $L = 15$ are shown in Figs 3(b) and 3(c), respectively. Figure 3(d) shows the result by using the local maximum and minimum velocities at depth levels. We can see that there are a large number of reference velocities even for low lateral

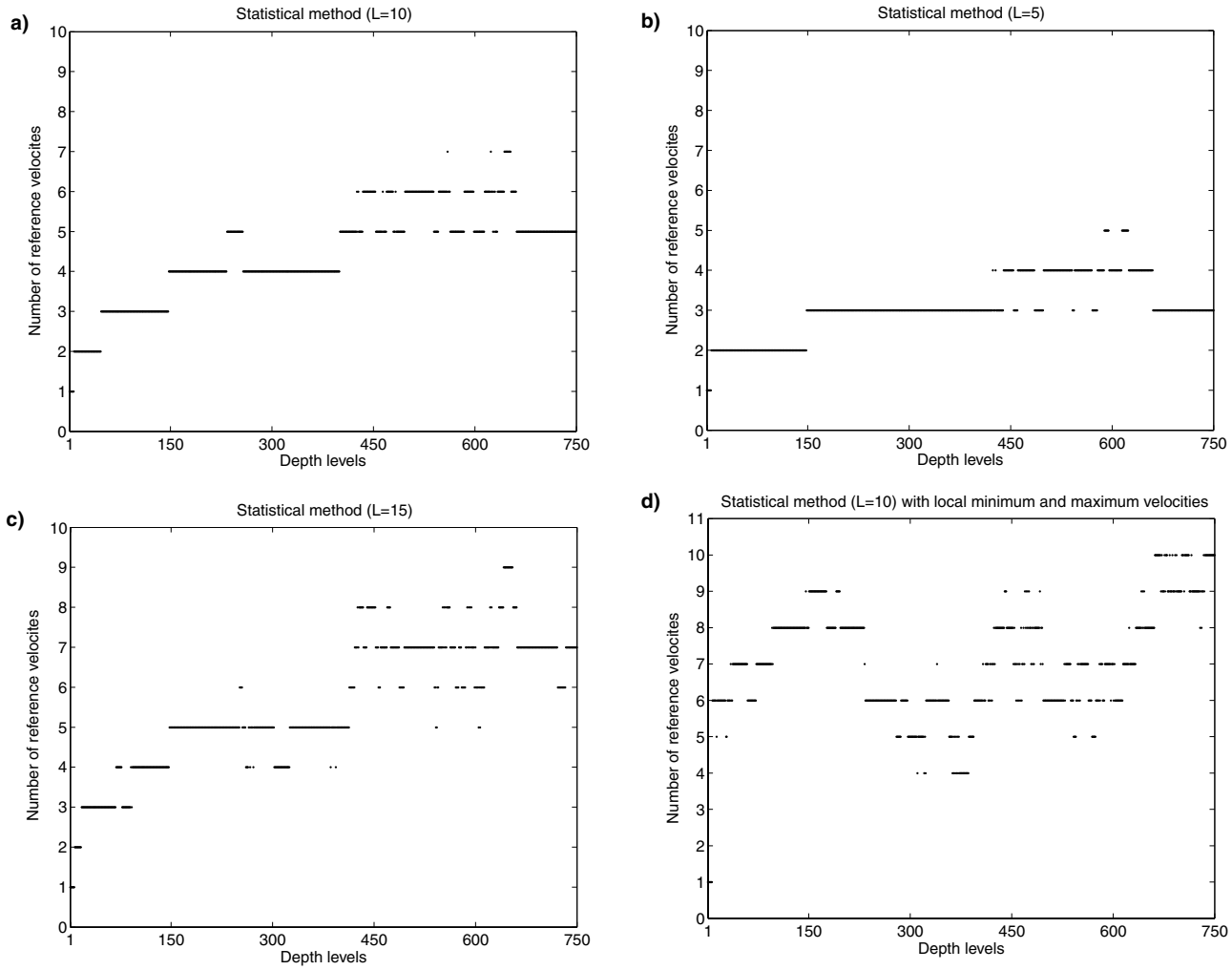

Figure 3 Statistical method for selecting reference velocities. (a) For $L = 10$; (b) for $L = 5$; (c) for $L = 15$; (d) for $L = 10$ but with local minimum and maximum velocities.

velocity variations, which is unnecessary. Therefore the statistical method should use the maximum and minimum velocities of the entire velocity model.

Now we make some comparisons between these two methods. For a given model, the number of reference velocities is determined by the common ratio ρ for the geometric progression method while for the statistical method it is determined by L. The geometric progression method is very simple but does not reflect the distribution of the velocities. On the other hand, the statistical method is relatively complicated but does account for the velocity distribution. Figure 4 shows the reference velocities for a particular depth determined by the geometric method (a) and the statistical method (b). For the geometric method, the reference velocities form a geometric progression. For the statistical method, the reference velocities reflect the velocity distribution where more reference velocities are concentrated on an area with high velocity distribution.

Next, we compare the imaging effect of PSPI and extended-split-step-Fourier on the Marmousi model. First, we use the statistical method to determine the reference velocities. We set $L = 10$. To begin with, we make a modification in the Han's statistical method. The statistical method uses the minimum and maximum velocities of the entire velocity model to define the number of reference velocities and uses the minimum velocity of the entire velocity as the first reference velocity at a depth level under consideration. We will use the minimum velocity at a depth level as the first reference velocity because it is more accurate in doing so. Figure 5 shows the migrated results. We can see that the results of PSPI (a) and extended-split-step-Fourier (b) are basically the same in terms of the

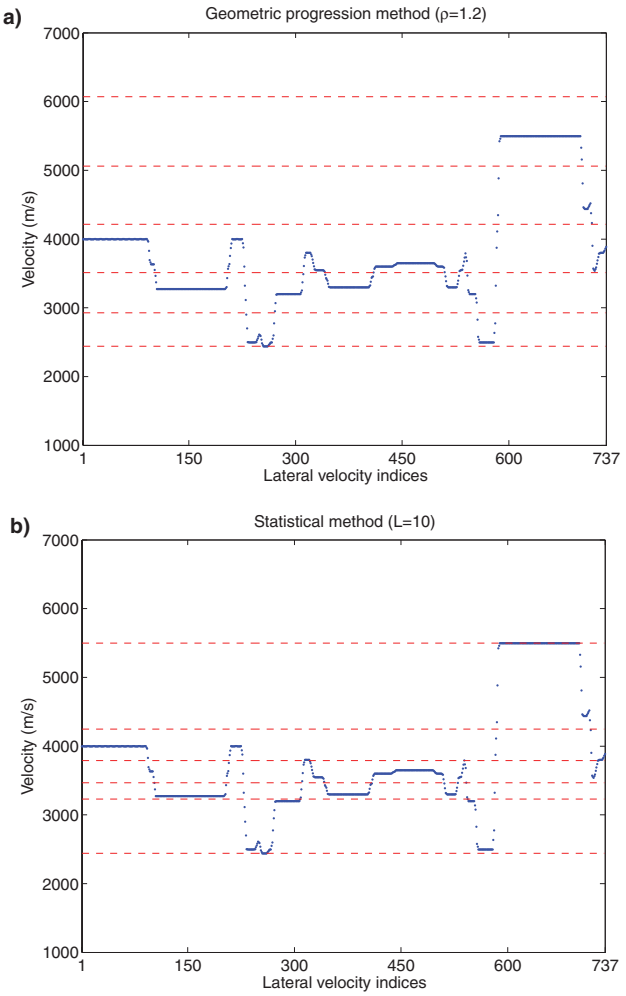

Figure 4 Reference velocities at a particular depth. The red dashed lines indicate the reference velocities. (a) Geometric progression method; (b) statistical method.

position and shape of reflectors and faults. This is in agreement with the theoretical analysis that both methods have the same kinematics properties. However the amplitudes calculated by these two methods are different. Figure 5(c) shows the amplitude difference of these two methods. In Fig. 6, we display the migration results by using the geometric progression method for selection of reference velocities. In this computation, we use $\rho = 1.2$. In this case, we can draw the same conclusion regarding the imaging results of PSPI and extended-split-step-Fourier.

In order to examine the results in Figs 5 and 6 more closely, seismic traces at two surface locations ($x = 5$ km and $x = 6.25$ km) are displayed in Fig. 7. From the traces, we can see that the traces of the PSPI and extended-split-step-Fourier methods indeed have the same phase that represents the kinematic characteristics of wave propagation, whereas their amplitudes differ from each other. For the influence of the choice of reference velocities, we can see that the traces obtained by the geometric progression method and the statistical method exhibit both phase and amplitude discrepancies.

CONCLUSIONS

Unified separable formulas of the PSPI and extended-split-step-Fourier methods are derived, which account for the three components of these methods: time-shift term, phase-shift with reference velocities and interpolation between wavefields. These formulas provide a concise and intrinsic understanding of these methods as a whole. Using these formulas, we show that these two methods have the same kinematic characteristics by means of the theory of pseudodifferential operators. Numerical experiments on the Marmousi model confirm the theoretical analysis. For the selection of reference velocities, we demonstrate that the geometric progression method is simple but does not take into account the velocity distribution, whereas the statistical approach is relatively complex but reflects the velocity distribution.

ACKNOWLEDGEMENTS

We would like to thank the anonymous reviewers for their careful and valuable suggestions. This work is supported by the National Natural Science Foundation of China under grant No. 40974074, 40774069 and 40830424.

REFERENCES

Bagaini C., Bonomi E. and Pieroni E. 1995. Data parallel implementation of 3-D PSPI. 65th SEG meeting, Houston, Texas, USA, Expanded Abstracts, 188–191.

Biondi B.L. 2006. *3-D Seismic Imaging*. SEG.

Chen J.-B. and Liu H. 2004. Optimization approximation with separable variables for the one-way wave operator. *Geophysical Research Letters* **31**, L06613.

Chen J.-B. and Liu H. 2006. Two kinds of separable approximations for the one-way operator. *Geophysics* **71**, T1–T5.

Chen J.-B., Liu H. and Zhang Z.F. 2007. A separable-kernel decomposition method for approximating the DSR continuation operator. *Geophysics* **72**, S25–S31.

Ferguson R.J. and Margrave G.F. 2005. Planned seismic imaging using explicit one-way operators. *Geophysics* **70**, S101–S109.

Gazdag J. and Sguazzero P. 1984. Migration of seismic data by phase shift plus interpolation. *Geophysics* **49**, 124–131.

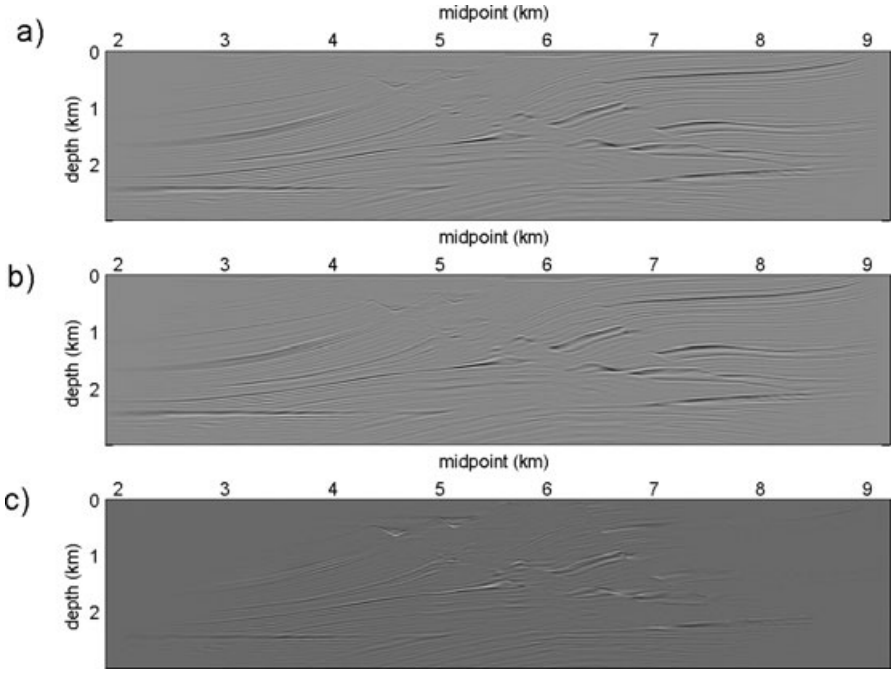

Figure 5 Migration results with PSPI and extended-split-step-Fourier by using the statistical method for selecting reference velocities. (a) PSPI; (b) extended-split-step-Fourier; (c) difference between PSPI and extended-split-step-Fourier.

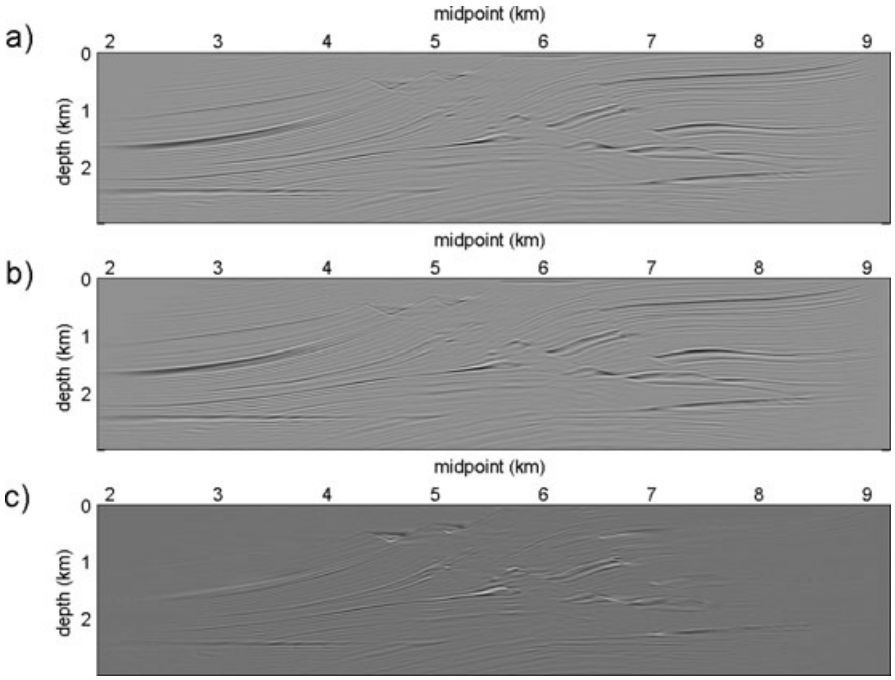

Figure 6 Migration results with PSPI and extended-split-step-Fourier by using the geometric progression method for selecting reference velocities. (a) PSPI; (b) extended-split-step-Fourier; (c) difference between PSPI and extended-split-step-Fourier.

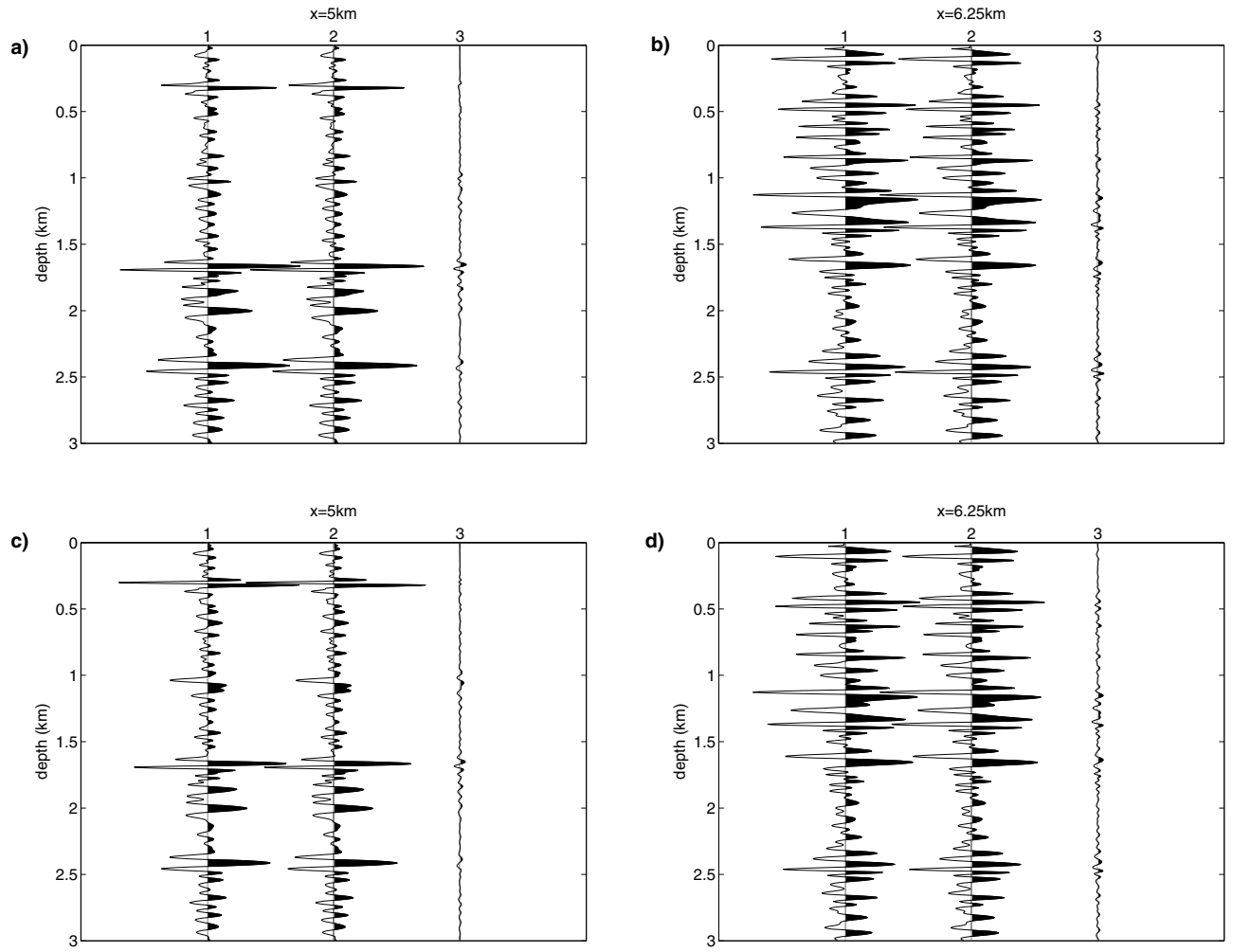

Figure 7 Seismic traces at two surface locations ($x = 5$ km and $x = 6.25$ km). "1" represents the PSPI method, "2" represents the extended-split-step-Fourier method, and "3" represents the difference between PSPI and extended-split-step-Fourier methods. (a) and (b) are obtained with the statistical method and (c) and (d) are obtained with the geometric progression method.

Gray S.H., Etgen J., Dellinger J. and Whitmore D. 2001. Seismic migration problems and solutions. *Geophysics* **66**, 1622–1640.

Han B.N. 1998. *A program for 2-D prestack common-shot phase-shift-plus-interpolation migration*. CWP/SU Free Software Package.

Hardy G.H., Littlewood J.E. and Pólya G. 1952. *Inequalities,* 2nd edn. Cambridge University Press.

Kessinger W. 1992. Extended split-step Fourier migration. 62nd SEG meeting, New Orleans, Lousiana, USA, Expanded Abstracts, 917–920.

Le Rousseau J.H., and de Hoop M.V., 2001. Modelling and imaging with the scalar generalized-screen algorithms in isotropic media. *Geophysics* **66**, 1551–1568.

Maslov V.P. and Fedoriuk M.V. 1981. *Semi-classical Approximation in Quantum Mechanics*. Reidel.

Stoffa P.L., Fokkema J.T., de Luna Freir R.M. and Kessinger W.P. 1990. Split-step Fourier migration. *Geophysics* **55**, 410–421.

Treves F. 1980. *Introduction to Pseudodifferential and Fourier Integral Operators, Vol. 1*. Plenum Press.

Zhang Y., Zhang G.Q. and Bleistein N. 2005. Theory of true-amplitude one-way wave equations and true-amplitude common-shot migration. *Geophysics*, **70** E1–E10.

APPENDIX

Some basic facts on pseudodifferential operators

In this appendix, we recall some concepts and results regarding pseudodifferential operators. For details, see Treves (1980) and Maslov and Fedoriuk (1981).

Let $L(\boldsymbol{x}, \boldsymbol{p}; \lambda)$ and $u(\boldsymbol{x})$ be scalar functions, where $\boldsymbol{x} = (x_1, x_2, \ldots, x_n)$, $\boldsymbol{p} = (p_1, p_2, \ldots, p_n)$, and λ is a parameter. With the

use of Fourier transformation, we can define two operators:

$$L(\overset{2}{\boldsymbol{x}}, \overset{1}{D_x}; \lambda)u(\boldsymbol{x}) = F^{-1}_{p\to x}\left[L(\boldsymbol{x}, \boldsymbol{p}; \lambda)F_{x\to p}u(\boldsymbol{x})\right], \tag{A1}$$

$$L(\overset{1}{\boldsymbol{x}}, \overset{2}{D_x}; \lambda)u(\boldsymbol{x}) = F^{-1}_{p\to x}\left[F_{x\to p}\left(L(\boldsymbol{x}, \boldsymbol{p}; \lambda)u(\boldsymbol{x})\right)\right], \tag{A2}$$

where $F_{x\to p}$ and $F^{-1}_{p\to x}$ are forward and inverse Fourier transforms, respectively and indices 1 and 2 indicate the order of the operators $\boldsymbol{x}$ and D_x when acting on a function, namely, which acts first and which acts second. Here

$$D_x = \left(\frac{1}{\mathrm{i}}\frac{\partial}{\partial x_1}, \ \frac{1}{\mathrm{i}}\frac{\partial}{\partial x_2}, \ \ldots, \ \frac{1}{\mathrm{i}}\frac{\partial}{\partial x_n}\right), \tag{A3}$$

where i is the imaginary unit.

The operators defined in (A1) and (A2) are called pseudodifferential operators and $L(\boldsymbol{x}, \boldsymbol{p}; \lambda)$ is their symbol.

For example, consider the wave equation in the frequency-space domain:

$$\left(\frac{\partial^2}{\partial x_1^2} + \frac{\partial^2}{\partial x_2^2} + \frac{\partial^2}{\partial x_3^2} + \frac{\omega^2}{v(x_1, x_2, x_3)^2}\right)u = 0, \tag{A4}$$

where u is the wavefield, ω is the circular frequency and $v(x_1, x_2, x_3)$ is the velocity.

For the Helmholtz operator in the parentheses in equation (A4), its symbol is

$$L(\boldsymbol{x}, \boldsymbol{p}; \lambda) = -(p_1^2 + p_2^2 + p_3^2) + \frac{\lambda^2}{v(x_1, x_2, x_3)^2}, \tag{A5}$$

where $\lambda = \omega$.

Let $S_1(\boldsymbol{x})$ and $S_2(\boldsymbol{x})$ be two real-valued functions. If, for any function $\varphi(\boldsymbol{x})$ with compact support, the following equations hold:

$$L(\overset{2}{\boldsymbol{x}}, \overset{1}{D_x}; \lambda)\left[\varphi(\boldsymbol{x})\exp(i\lambda S_1(\boldsymbol{x}))\right] = O(\lambda^{-1}), \quad \lambda \to +\infty, \tag{A6}$$

$$L(\overset{1}{\boldsymbol{x}}, \overset{2}{D_x}; \lambda)\left[\varphi(\boldsymbol{x})\exp(i\lambda S_2(\boldsymbol{x}))\right] = O(\lambda^{-1}), \quad \lambda \to +\infty, \tag{A7}$$

then we call $S_1(\boldsymbol{x})$ and $S_2(\boldsymbol{x})$ the characteristics associated with $L(\overset{2}{\boldsymbol{x}}, \overset{1}{D_x}; \lambda)$ and $L(\overset{1}{\boldsymbol{x}}, \overset{2}{D_x}; \lambda)$, respectively. The characteristic of a pseudodifferential operator satisfies the corresponding Hamilton-Jacobi equation. In the case of the scalar wave equation where $\lambda = \omega$, the Hamilton-Jacobi equation becomes the eikonal equation and the characteristic becomes the traveltime function (Maslov and Fedoriuk 1981). Specifically, the Hamiltonian-Jacobi equation for equation (A4) is

$$\left(\frac{\partial T}{\partial x_1}\right)^2 + \left(\frac{\partial T}{\partial x_2}\right)^2 + \left(\frac{\partial T}{\partial x_3}\right)^2 = \frac{1}{v(x_1, x_2, x_3)^2}, \tag{A8}$$

where $T(x_1, x_2, x_3)$ is the travel time. The equation (A8) is just the eikonal equation.

An important result about the characteristics is that the characteristics $S_1(\boldsymbol{x})$ and $S_2(\boldsymbol{x})$ defined in (A6) and (A7) coincide, namely $S_1(\boldsymbol{x}) = S_2(\boldsymbol{x})$ (Proposition 3.6, in Maslov and Fedoriuk 1981).